



The Compact Muon Solenoid Experiment
Conference Report

Mailing address: CMS CERN, CH-1211 GENEVA 23, Switzerland



24 November 2016 (v2, 28 November 2016)

Commissioning of Upgrade Forward Hadron Calorimeters of CMS

Burak Bilki for the CMS Collaboration

Abstract

The CMS experiment at the Large Hadron Collider (LHC) at CERN is upgrading the photo-detection and readout system of the forward hadron calorimeter (HF). During Long Shutdown 1, all of the original PMTs were replaced with multi-anode, thin window photomultipliers. At the same time, the back-end readout system was upgraded to micro-TCA readout. Here we report on the experience with commissioning and calibrating the HF front-end as well as the online operational challenges of the micro-TCA system.

Presented at *IEEE-NSS-MIC-2016 IEEE Nuclear Science Symposium and Medical Imaging Conference*

Commissioning of Upgrade Forward Hadron Calorimeters of CMS

Burak Bilki

On behalf of the CMS Collaboration

Abstract—The CMS experiment at the Large Hadron Collider at CERN is upgrading the photodetector and readout system of the forward hadron calorimeter. During Long Shutdown 1, all of the original photomultiplier tubes were replaced with multi-anode, thin window photomultipliers. At the same time, the back-end electronics were upgraded to μ TCA-based readout. Here we report on the commissioning, operations and near future plans of the forward hadron calorimeters Phase I Upgrade.

I. INTRODUCTION

The forward hadron calorimeter (HF) of the Compact Muon Solenoid (CMS) [1] experiment at the CERN Large Hadron Collider (LHC) covers the pseudorapidities (η) between 3 and 5. The HF calorimeters on both sides are located at 11.2 m from the interaction point. The signal in the HF calorimeter originates from the Čerenkov light emitted in the quartz fibers which are embedded in a large steel structure. The diameter of the quartz fibers is 0.6 mm and they are placed 5 mm apart in a square grid. The quartz fibers run parallel to the beam line and have two different lengths (1.43 m and 1.65 m), creating two effective longitudinal samplings. The short fibers are mostly sensitive to hadron interactions. There are 13 towers in η , and the ϕ segmentation of all towers is 10° , except for the highest- η . This leads to 900 towers and 1800 channels in the two HF calorimeter modules [2]. The readout of the bundled fibers is provided with photomultiplier tubes (PMTs). The PMTs are placed into magnetic shields and are coupled to air light guides. Figure 1 shows a sketch of the CMS hadron calorimeters. Figure 2 shows a close-up sketch of the HF calorimeter. Details of the HF calorimeter design, together with beam test results and calibration methods, can be found in [3].

The HF calorimeters have a crucial role in physics measurements particularly in forward jet tagging in Higgs mass reconstruction and the calculation of the missing transverse energy. There are several possible Higgs production mechanisms. Two of the more prominent methods are gluon fusion and vector boson fusion. Gluon fusion processes are expected to be the dominant mechanism. Vector boson fusion, however, has a feature which makes it a favorable discovery channel: forward jets. In vector boson fusion, two quarks radiate virtual W or Z bosons, which in turn inverse decay (or fuse) to produce a Higgs boson. The Higgs boson itself is not directly detectable. Instead, it is the decay products of the Higgs which are identified and reconstructed to form the hypothesis of

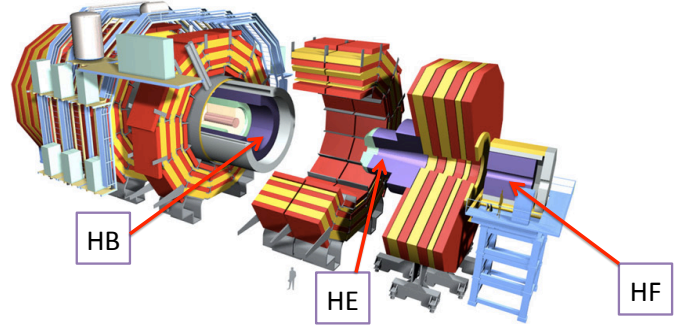


Fig. 1. A sketch of the CMS detector highlighting the hadron calorimeters: Barrel (HB), endcap (HE) and forward (HF).

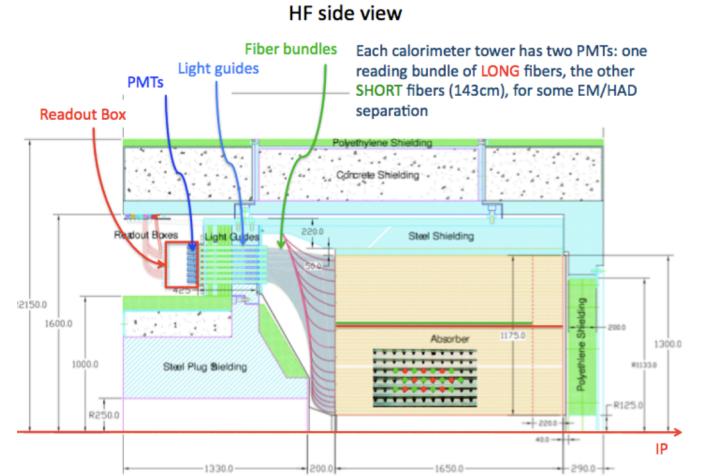


Fig. 2. A sketch of the CMS HF calorimeter.

the Higgs Boson. CMS measurements of the Higgs boson are primarily focused on five decay channels: $H \rightarrow \gamma\gamma$, $H \rightarrow ZZ^* \rightarrow 4l$, $H \rightarrow WW^*$, $H \rightarrow \tau\tau$, and $H \rightarrow b\bar{b}$. If $H \rightarrow \tau\tau$ channel is considered with the specific case where both τ particles decay leptonically, which means that each τ decays to an electron or muon and respective neutrinos, Fig. 3 shows the distributions of pseudorapidities of the tagged jets. As can be seen, a significant fraction of the jets are within the HF calorimeter coverage $3 < |\eta| < 5$.

II. NEED FOR AN UPGRADE

The PMTs of the HF calorimeter during Run I were Hamamatsu R7525 [4], [5] PMTs. The PMTs have circular windows with 2.54 cm diameter and 2 mm thickness at the center that gets thicker towards the rim. These PMTs generate a large,

Manuscript received on November 30, 2016.

Burak Bilki is with the University of Iowa, Iowa City, IA, USA and Beykent University, Istanbul, Turkey, e-mail: Burak.Bilki@cern.ch.

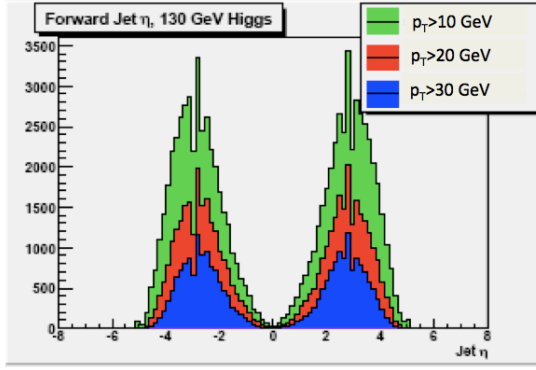


Fig. 3. Distributions of pseudorapidities of jets from $qqH \rightarrow \tau\tau \rightarrow leptons$.

fake signal when the PMT window is traversed by a relativistic charged particles due to Čerenkov light production at the PMT window. This already-known problem was observed in the 2010 and 2011 CMS data to degrade data quality dramatically and to constitute a potential to interfere with rare physics events. Figure 4 shows the muon response of HF R7525 PMTs at 150 GeV Muon test beam. The peak around 200 GeV is due to muons interacting with the PMT and the peak around 4 GeV is for muons interacting with the HF detector itself. The phenomenon was extensively studied in beam tests with various types of PMTs at a later stage [6].

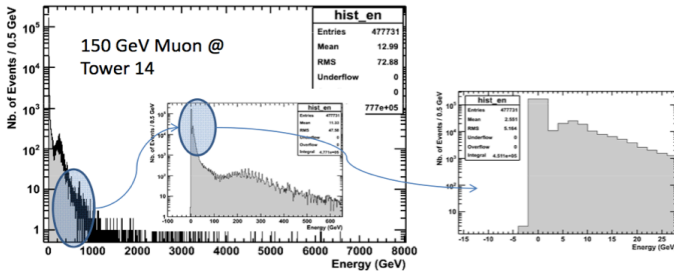


Fig. 4. Muon response of the HF calorimeter as well as the R7525 PMTs at 150 GeV test beam.

III. THE COMPONENTS OF THE PHASE I UPGRADE

A. Upgrade PMTs

During the first long shutdown (LS1) in 2013-2014, the PMTs in HF (Hamamatsu R7525) were replaced with Hamamatsu R7600U-200-M4 PMTs [5]. The upgrade PMTs utilize thinner windows, four anode segments, basic properties exceeding the HF requirements. The thinner windows and the metal envelope reduce the size and rate of the window events. Multi-anode feature allows the tagging and recovery of events with background. High quantum efficiency and gain offer an improved HF performance. The meshed structure makes the PMT less susceptible to magnetic field. New multi-anode PMTs have four anodes, thinner window (< 1 mm) and a metal envelope. Their characterisations at 800 V are high quantum efficiency (38 - 39 %), high gain ($> 10^6$), low dark current (< 1 nA) and fast timing (rise time < 2 ns, transit time < 25 ns and pulse width < 15 ns) [7].

The characterization tests of new PMTs were done at the University of Iowa PMT test station. Each PMT was tested for gain, dark current and timing at the range of operating voltages 600 - 900 V in increments of 50 V.

Figure 5 shows the gain (top) and dark current (bottom) distributions of R7600U-200-M4 PMTs at 800 V. The mean (RMS) of gain and dark current respectively are 2.44×10^6 (1.19×10^6) and 0.665 (0.770) nA.

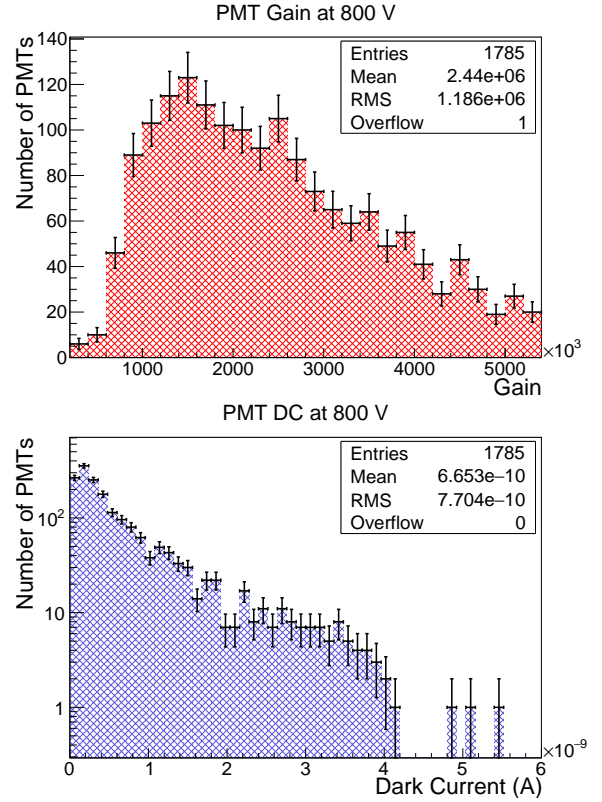


Fig. 5. Gain (top) and dark current (bottom) distributions for R7600U-200-M4 PMTs at 800 V.

The upgrade PMT does not only reduce the intrinsic level of the background, but it also enables tagging of background events and recovering the underlying signal event (if any) by using the multi-anode features. For the calorimeter signal, the quad anode PMT views the well-mixed light from the air light guide, thus all 4 anodes should have the same signal (up to statistical variations). However, a MIP background affects one quadrant (or one half) of the PMT, thus generating increased anomalous signals in one of the readout channels but not the others. The background from a MIP may thus be tagged by various algorithms (which have already been studied extensively [6], [8]) comparing the anode signals; if the signals are sufficiently different, we can assume a background MIP causes it. Once an anode with a background is tagged, the signal can be recovered by using only the signals in the other anode(s).

The beam test results indicate that the R7600U-200-M4 offers reduced rate and lower response to muon incidence on PMT windows at any angle of incidence when compared to R7525. The equivalent energy response to traversing MIP backgrounds is lowered by more than a factor of 5 in R7600U-

200-M4. The response to the real calorimeter Čerenkov signals by the R7600U-200-M4 is more than 2 times higher than R7525 response (this response enables usable muon response, provides better signal-to-noise ratio, and gives a stochastic term in the energy resolution 45% smaller/better). A simple algorithm for identifying PMT window events and recovering the signal, utilizing multi-channels of the R7600U-200-M4, has been demonstrated with the test beam data. The algorithm is >90% efficient in identifying events with direct muon incidence on PMT windows, and reduces the rate of background events by a factor of about 20. The algorithm corrects the energy of real events with a MIP background to the true energy, within a few percent.

B. Readout Boards

HF requires 72 readout boxes, 216 baseboards with 1728 PMTs, and the ability for each 4-anode PMT to be read out in 1 or 2 channel operations. This design challenge was met with a single PMT board, the so-called base board, and multiple adapter boards. Figure 6 shows the pictures of the readout box (top) and the base and adapter boards (bottom). From LS1 until the end of 2016, the PMTs were read out in 1-channel mode. During the Extended Year End Technical Stop 2016 - 2017 (EYETS 16-17), the 1-channel adapter boards will be replaced with the 2-channel adapter boards. The readout box shown in Fig. 6 is in assembly for the 1-channel mode. The cables needed for the 2-channel readout can be seen as tied bundles.

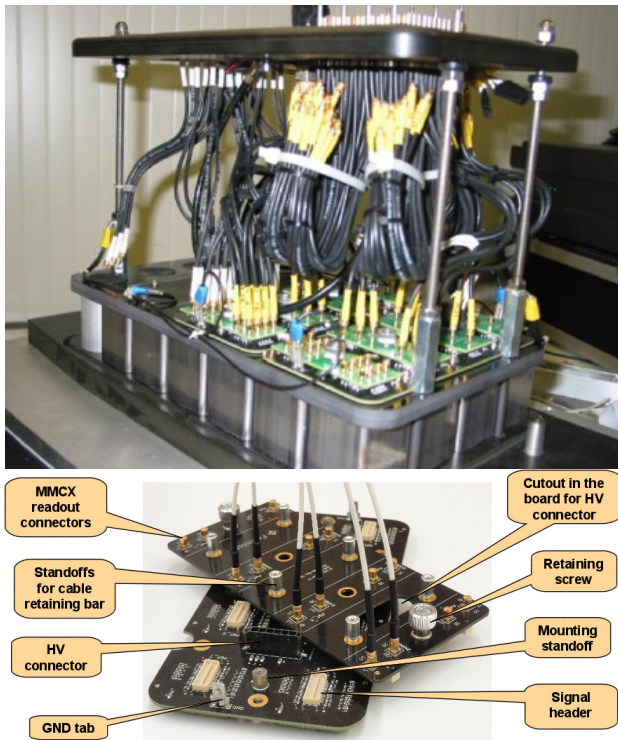


Fig. 6. (a) Picture depicting the HF readout box anatomy during assembly. The PMTs appear inverted on the table. The base boards, adapter boards and internal cabling are also visible. The entire box can read out 24 PMTs in three front-end electronics boards. (b) Picture of the base (bottom) and adapter (top) boards before assembly. Major parts of the boards are labeled.

The R7600 baseboard has 8 power supplies (1 per PMT) with 3 sets of independent voltages (Vpc, Vd9, Vd10). The design incorporates conventional resistive bases, provides reference signals for the charge integrator encoder (QIE) readout card, and supplies ground connections to the PMT shields.

In order to comply with the different phases of the upgrade program, the adapter board is designed to provide convenient switching between different readout options. The adapter board uses through hole mounted MMCX (micro miniature coaxial) signal connectors. There are screw/standoff retainers for attachment to the base board.

C. Front-end Electronics

An updated QIE, called QIE10 has been designed to digitize the PMT signal and the signals arrival time information. It features deadtimeless integration and digitization of charge in 25 ns ‘buckets’; the same clock as the LHC.

On board is a rising edge TDC with a resolution of less than 800 ps, which outputs a discrimination bit. It has a large dynamic range of 3 fC to 330 pC and holds this information in 17 bits. Its digitization error is less than the calorimeter resolution and is at the order of 2-3 %, held in 6 bits. It digitizes in 4 ranges, stored in 6-bit mantissa and 2-bit exponent. It matches the input impedance of the new PMTs.

Figure 7 shows the distribution of leading edge TDC versus ADC for a single QIE10 channel. The data is collected during CMS Run II operations. The figure shows two clusters of points: one around TDC 30 and another around TDC 16. The later events are consistent with signals from particle showers. The earlier events are consistent with noise from particles incident on quartz PMT windows. Further studies are in progress to better characterize these events. The multi-anode features will enable the recovery of the signal with more than 90 % efficiency.

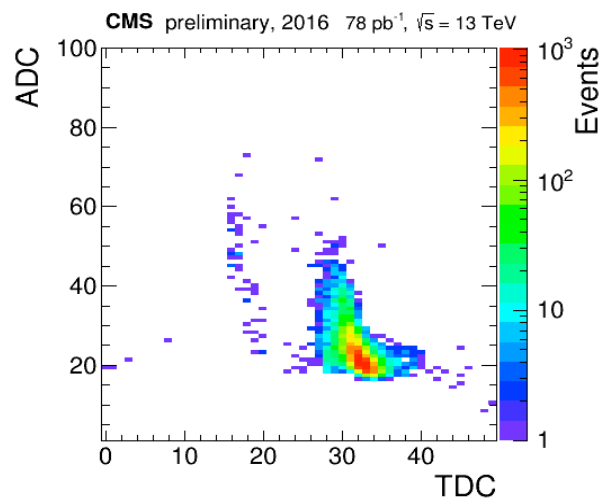


Fig. 7. The distribution of leading edge TDC versus ADC for a single QIE10 channel.

A major design consideration was the intense radiation environment of the High Luminosity LHC. The QIE10 features a radiation tolerant FPGA (ProASIC3E from Microsemi)

manufactured using the AMS 0.35-micrometer SiGe BiCMOS process. This FPGA is responsible for synchronizing and formatting the data from several QIEs. It also determines the pulse width from the time discriminator output. The chip is tolerant to 100 Gy, though it is expected to receive a total ionizing dose of 1.5 Gy.

A new data link was developed by CERN to carry this information to the counting room. GBTx is a 4.8 Gbps data link that serializes the QIE10 data for transmission to the back-end electronics. 88 bits of user data can be carried every bunch crossing.

An important benefit of the ADC card design is that it will be possible to reformat the data if required through reprogramming of the FPGA. As an example, this would allow the reorganization of the data if an optical link failed and a replacement would not be possible for some time.

A large-scale test station has been established to test all the QIE10 cards before installation in CMS. Figure 8 shows a picture of the test station. The QIE10 cards pass through acceptance, calibration and LED tests successively. Once the cards qualify, they are placed in the burn-in station for long-term stability tests.

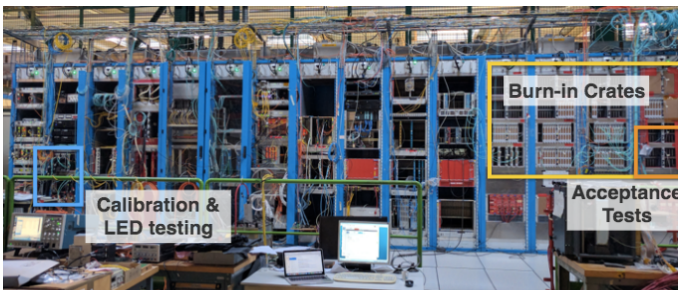


Fig. 8. The QIE10 cards test station.

D. Back-end Electronics

The upgraded electronics take advantage of a new industrial standard known as μ TCA. This crate standard replaced the existing VME crate system. The new electronics improve the noise rejection and the granularity of the HF readout and trigger. Figure 9 shows the crate layout structure of the μ TCA-based back-end electronics [9]. The crate contains 4 components: Power Module, MCH (μ TCA carrier hub), μ HTR/ μ CTR (mini CMS Trigger Readout), AMC13/DTC (DAQ and Timing Card). The new modules allow an increased data transfer rate; can receive data via a high-speed 5 Gbps asynchronous link and record histograms with LHC bunch crossing time resolution.

The μ TCA standard has explicit support for the hot-swapping of AMCs. When an AMC is inserted into the μ TCA crate, the MCH communicates via the I2C protocol with a sub-component of the AMC called the Mezzanine Management Controller (MMC). After a successful negotiation, including the information that sufficient electrical power will be available, the 12 V payload power to the AMC is turned on by the MCH. The communication between the MCH and MMC is also used for monitoring voltages, currents, and temperatures

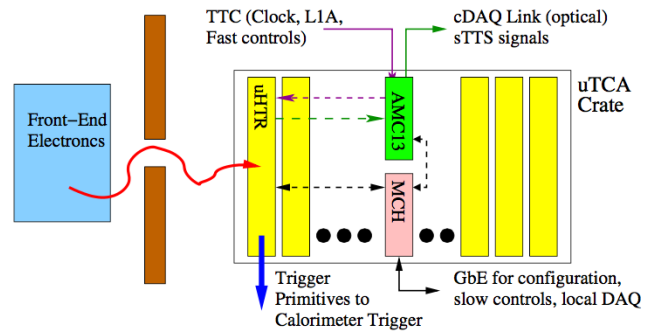


Fig. 9. Crate layout structure of the μ TCA-based back-end electronics.

on the AMC card. Additionally, low-level configuration of the card can be performed over this link, including providing the card with its crate identifier. Besides the slow-control I2C link, each MCH site has multiple high-speed serial pairs connecting to the AMC slots. One of these is used for a Gigabit Ethernet (GbE) link which is the primary communication path for configuration and monitoring in a μ TCA crate. Several connections are used for the distribution of clock signals in the crate, and each MCH site has at least four bi-directional high-speed serial connections to each AMC slot. In the μ TCA standard, the protocol to be used on these additional ports is a user-specified condition.

IV. CONCLUSIONS

The CMS Forward Hadron Calorimeters have been going through a photodetector, as well as front-end and back-end electronics upgrade. The new multi-anode PMTs have low dark currents (below 1 nA) and high gain (above 10^6). They show fast timing characteristics with a rise time of less than 3 ns, transit time and pulse width less than 6 ns. They operate stably and are now being used to collect data at the CMS experiment. These PMTs with all the improved specifications overcome large energy window event issues in the HF calorimeter, reduce fake background and make the experiment more efficient. New back-end electronics based on μ TCA provide increased data transfer rate. Also, upgrade front-end electronics, QIE10, will provide wider dynamic range and incorporate TDC functionality. During the Extended Year End Technical Stop 2016 - 2017, the PMTs will be switched to the 2-channel readout mode by changing the adapter boards inside the readout boxes, and the front-end electronics will be installed.

REFERENCES

- [1] S. Chatrchyan et al. (CMS collaboration), JINST 3 S08004, 2008.
- [2] G. L. Bayatian et al. (CMS collaboration), CERN/LHCC-2006-001, 2006.
- [3] P. Adzic et al. (CMS ECAL Collaboration), Eur. Phys. J. C 44 1-10, 2006.
- [4] P. Adzic et al. (CMS ECAL Collaboration), JINST 2 P04004, 2007.
- [5] <http://www.hamamatsu.com/>.
- [6] S. Chatrchyan et al. (CMS HCAL collaboration), JINST 5 P06002, 2010.
- [7] U. Akgun et al., JINST 9 T06005, 2014.
- [8] S. Chatrchyan et al. (CMS HCAL collaboration), JINST 7 P10015, 2012.
- [9] CMS Collaboration, Technical Report CERN-LHCC-2011-006, CERN, Geneva, June 2011.